

# Self Regulated AGN Interaction with Cluster Cooling Core Regions: The Metallicity Distribution as Diagnostics

H. Böhringer,<sup>1</sup> K. Matsushita,<sup>1,2</sup> E. Churazov,<sup>3</sup> and A. Finoguenov<sup>1</sup>

<sup>1</sup> *Max-Planck-Institut für extraterr. Physik, D 85748 Garching, Germany*

<sup>2</sup> *Tokyo University of Science, Tokyo, Japan*

<sup>3</sup> *Max-Planck-Institut für Astrophysik, D 85748 Garching, Germany*

The X-ray observations with XMM-Newton show a lack of spectral evidence for large amounts of cooling and condensing gas in the centers of galaxy clusters believed to harbor strong cooling flows. These findings lead to a revision of our understanding of so-called cooling flows. To explain these findings we consider the heating of the core regions of clusters by jets from a central AGN. The requirements such a heating model has to fulfill are explored and we find a very promising scenario of self-regulated Bondi accretion of the central black hole.

XMM-Newton observations of the central regions of clusters of galaxies also provide detailed information on the distribution of up to 8 heavy elements. In cooling core clusters a strong abundance is usually observed towards the center. From the elemental composition we conclude that most of these metals originate from supernovae type Ia. Here we discuss the implications of the observed cumulative mass profiles of these metals. We find that long enrichment times ( $\geq 7$  Gyr) are necessary to produce these central abundance peaks. Classical cooling flows, a strongly convective intracluster medium, and a complete metal mixing by cluster mergers would destroy the observed abundance peaks too rapidly. Thus the observations set strong constraints on cluster evolution models requiring that the cores of cooling core clusters are preserved over very long times.

## 1. Introduction

X-ray imaging observations have shown that the X-ray emitting, hot gas in a large fraction of all galaxy clusters reaches high enough densities in the cluster centers that the cooling time of the gas falls below the Hubble time, and gas may cool and condense in the absence of a suitable fine-tuned heating source (e.g., Silk 1976, Fabian & Nulsen 1977). From the detailed analysis of surface brightness profiles of X-ray images of clusters obtained with the *Einstein*, *EXOSAT*, and *ROSAT* observatories, the detailed, self-consistent scenario of inhomogeneous, co-moving cooling flows emerged (e.g., Nulsen 1986, Thomas, Fabian, & Nulsen 1987, Fabian 1994). The main assumptions on which the cooling flow model is based and some important implications are: (i) Each radial zone in the cooling flow region comprises different plasma phases covering a wide range of temperatures. The consequence of this temperature distribution is that gas will cool to low temperature and condense over a wide range of radii. (ii) The gas features an inflow in which all phases with different temperatures move with the same flow speed. (iii) There is no energy exchange between the different phases, between material at different radii, and no heating.

High resolution X-ray spectra and imaging spectroscopy obtained with XMM-Newton has shown to our surprise that the spectra show no signatures of cooler phases of the cooling flow gas below an intermediate tem-

perature (e.g., Peterson et al. 2001, Tamura et al. 2001). We also observed approximate local isothermality in the cooling flow region (e.g., Böhringer et al. 2001b, Matsushita et al. 2002, Molendi & Pizzolato 2001) in conflict with the inhomogeneous cooling flow model. Here, we discuss the information obtained on the thermal structure of cluster centers, mostly for the example of M87, as obtained from the analysis of spectro-imaging data with the X-ray CCD detectors of XMM-Newton. We also review the prospects of the AGN heating models and discuss to which degree the requirements of a successful heating model are consistent with the observations.

The abundance distribution of several important heavy elements, which can for the first time be studied in detail with XMM-Newton, can be used as diagnostics of the thermal and dynamical history of the cooling core regions. We discuss the detailed implications of XMM-Newton abundance studies for four nearby cooling core clusters and find that cooling cores are old structures which have to be well preserved over most of the cluster lifetime.

## 2. Spectroscopic Diagnostics of Cooling Cores

XMM Reflection Grating Spectrometer (RGS) observations of several cooling core regions show signatures of different temperature phases ranging approximately from the hot virial temperature of the cluster to a lower limiting temperature,  $T_{low}$ . Clearly observable spectroscopic features of even lower temperature gas expected for a

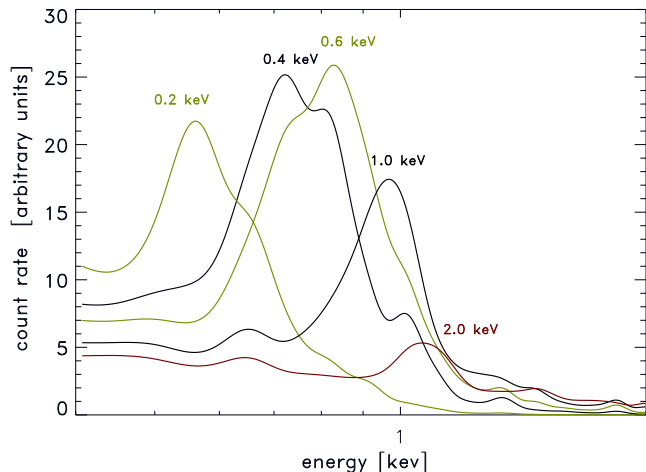


FIG. 1.— The Fe L-line complex in X-ray spectra as a function of the plasma temperature for a metallicity value of 0.7 solar. The simulations show the appearance of the spectra as seen with the XMM EPN. The emission measure was kept fixed when the temperature was varied.

cooling flow model are not observed (Peterson et al. 2001, Tamura et al. 2001, Kaastra et al. 2003). These results are very well confirmed by XMM observations with the energy sensitive imaging devices, EPN and EMOS. They are in addition providing spectral information across the entire cooling core region, yielding the result that (for M87, A1795, and A1835) single temperature models provide a better representation of the data than cooling flow models (Böhringer et al. 2001a, Molendi & Pizzolato 2001) also implying the lack of low temperature components. The very detailed analysis of M87 by Matsushita et al. (2002) has shown that the temperature structure is well described locally by a single temperature over most of the cooling core region, except for the regions of the radio lobes and the very center ( $r \leq 1'$ ,  $\sim 5$  kpc).

Among the spectroscopic signatures which are sensitive to the plasma temperature in the relevant temperature range, the complex of iron L-shell lines is most important. Fig. 1 shows simulated X-ray spectra as predicted for the XMM EPN instrument in the spectral region around the Fe L-shell lines for a single-temperature plasma at various temperatures from 0.4 to 2.0 keV and 0.7 solar metallicity. There is a very obvious shift in the location of the peak making this feature an excellent thermometer. For a cooling flow with a broad range of temperatures one expects a composite of several of the relatively narrow line blend features, resulting in a quite broad peak. Fig. 2a shows for example the deprojected spectrum of the M87 halo plasma for the radial range 1–2' (outside the inner radio lobes) and a fit of a cooling flow model with a mass deposition rate slightly less than  $1 M_{\odot} \text{ yr}^{-1}$  as expected for this radial range from the analysis of the surface brightness profile (e.g., Matsushita et al. 2001). It is evident that the peak in the cooling flow model is much broader than the observed spectral feature. For comparison Fig. 2b shows the same spectrum fitted by a cooling flow model where a temperature of 2 keV was chosen for the maximum temperature

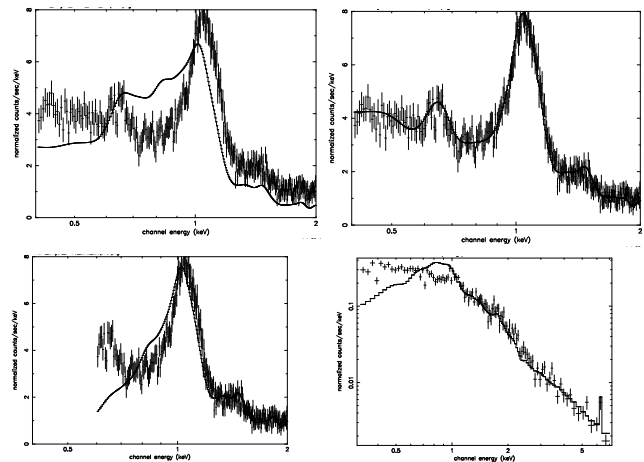


FIG. 2.— XMM EPN spectrum of the M87 X-ray halo in the radial range  $R = 1-2'$ . The spectrum has been fitted with a cooling flow model with a best fitting mass deposition rate of  $0.96 M_{\odot} \text{ yr}^{-1}$  and a fixed absorption column density of  $1.8 \times 10^{20} \text{ cm}^{-2}$ , the Galactic value, and a parameter for  $T_{low}$  of 0.01 keV. **(b - upper right)**: same spectrum fitted by a cooling flow spectrum artificially constrained to emission from the narrow temperature interval 1.44–2.0 keV, where  $T_{low}$  was treated as a free fitting parameter. **(c - lower left)**: same spectrum fitted with a free parameter for the internal excess absorption. The spectrum was constrained to the energy interval 0.6 to 2.0 keV. **(d - lower right)**: XMM EPN spectrum of A1795 fitted with a cooling flow model with the Galactic value for absorption.

and a suitable lower temperature cut-off (1.44 keV) was determined by the fit. The very narrow temperature interval (almost isothermality) is well consistent with the narrow peak. A similar result is obtained for other clusters, e.g., A1795 as shown in Fig. 2d.

Since this diagnostics of the temperature structure is essentially based on the observation of metal lines, an inhomogeneous distribution of the metal abundances in the cluster ICM and a resulting suppression of line emission at low temperatures was suggested as a possible way to reconcile the above findings with the standard cooling flow model by Fabian et al. (2001). As shown by Böhringer et al. (2002) such a scenario will still result in a relatively broad Fe L-line feature and does not solve the problem in this case of M87.

### 3. Internal Absorption

Another possible attempt to obtain consistency in the fit of the observed spectra with cooling flow models is to allow the absorption parameter in the fit to adjust freely. This is demonstrated in Fig. 2c with the same observed spectrum where the best fitting absorption column density is selected in such a way by the fit that the absorption edge limits the extent of the Fe-L line feature towards lower energies. This is actually the general finding with ASCA observations showing two possible options for the interpretation of the spectra of cluster core regions: (1) an interpretation of the results in form of an inhomogeneous cooling flow model which then necessarily includes an internal absorption component (e.g., Allen 2000, Allen et al. 2001), or (2) an explanation of the spectra in terms of a two-temperature component model

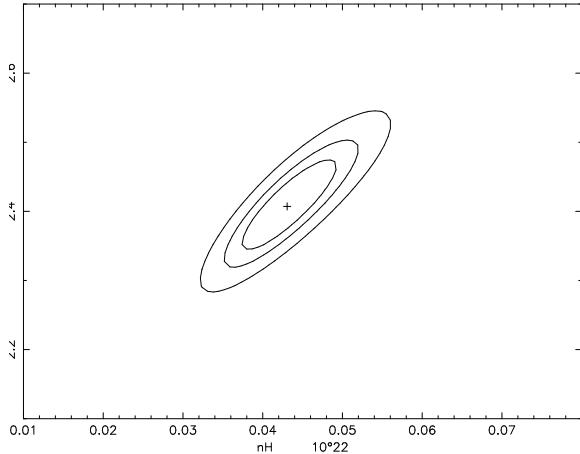


FIG. 3.— Constraints on the shape of the *XMM EPN*-spectrum of the nucleus of M87. The lines show the 1, 2, and  $3\sigma$  confidence intervals for the combined fit of the slope (photon index) of the power law spectrum and the value for the absorbing column density,  $n_H$ , in units of  $10^{22} \text{ cm}^{-2}$ .

(e.g., Ikebe et al. 1999, Makishima et al. 2001) where the hot component is roughly equivalent to the hot bulk temperature of the clusters and the cool component corresponds approximately to  $T_{low}$ . Thus for the cooling flow interpretation to work and to produce a sharp Fe-L line feature as observed, the absorption edge has to appear at the right energy and therefore values for the absorption column of typically around  $3 \times 10^{21} \text{ cm}^{-2}$  are needed (e.g., Allen 2000 and Allen et al. 2001 who find values in the range  $1.5\text{--}5 \times 10^{21} \text{ cm}^{-2}$ ).

It is therefore important to perform an independent test on the presence of absorbing material in the cluster cores. Thanks to *CHANDRA* and *XMM-Newton* we can now use central cluster AGN as independent light sources for probing. Using the nucleus and jet of M87 (with *XMM*, see Fig. 3) and the nucleus of NGC1275 (with *CHANDRA*) we find no signature of internal absorption. Thus at least for these two cases internal absorption is not observed.

#### 4. Heating Model

In view of these difficulties of interpreting the observations with the standard cooling flow model, we may consider the possibility that the cooling and mass deposition rates are much smaller than previously thought, that is reduced by at least one order of magnitude. To decrease the mass condensation under energy conservation some form of heating is clearly necessary. Three forms of heat input into the cooling flow region have been discussed: (i) heating by the energy output of the central AGN (e.g., Pedlar et al. 1990, Tabor & Binney 1993, McNamara et al. 2000, (ii) heating by heat conduction from the hotter gas outside the cooling flow (e.g., Tucker & Rosner 1983, Bertschinger & Meiksin 1986), and (iii) heating by magnetic fields, basically through some form of reconnection (e.g., Soker & Sarazin 1990, Makishima et al. 2001). The latter two processes depend on poorly known plasma physical conditions and are thus more speculative. The energy output of the central AGN, however, can be de-

termined as shown below.

A heating scenario can only successfully explain the observations if among others the two most important requirements are met: (i) the energy input has to provide sufficient heating to balance the cooling flow losses, that is about  $10^{60}$  to  $10^{61}$  erg in 10 Gyr or on average about  $3 \times 10^{43} - 3 \times 10^{44} \text{ erg s}^{-1}$ , and (ii) the energy input has to be fine-tuned. Too much heating would result in an outflow from the central region and the central regions would be less dense than observed. Too little heat will not reduce the cooling flow by a large factor. Therefore the heating process has to be self-regulated: mass deposition triggers the heating process and the heating process reduces the mass deposition.

Further constraints are discussed by Böhringer et al. (2002). The total energy input into the ICM by the relativistic jets of the central AGN can be estimated by the interaction effect of the jets with the ICM by means of the scenario described in Churazov et al. (2000, 2002). It relies on a comparison of the inflation and buoyant rise time of the bubbles of relativistic plasma which are observed, e.g., in the case of NGC 1275 (Böhringer et al. 1993, Fabian et al. 2000). The estimated total energy output is for three examples, M87:  $1.2 \times 10^{44} \text{ erg s}^{-1}$ , Perseus:  $1 \times 10^{45} \text{ erg s}^{-1}$ , and Hydra A:  $2 \times 10^{45} \text{ erg s}^{-1}$ . These values for the energy input have to be compared with the energy loss in the cooling flow, which is of the order of  $10^{43} \text{ erg s}^{-1}$  for M87 and about  $10^{44} \text{ erg s}^{-1}$  for Perseus. Thus in these cases the energy input is larger than the radiation losses in the cooling flow for at least about the last  $10^8$  yr. We have, however, evidence that this energy input continued for a longer time with evidence given by the outer radio halo around M87 with an outer radius of 35–40 kpc (e.g., Kassim et al. 1993, Rottmann et al. 1996). Owen et al. (2000) give a detailed physical account of the halo and model the energy input into it. They estimate the total current energy content in the halo in form of relativistic plasma to  $3 \times 10^{59} \text{ erg}$  and the power input for a lifetime of about  $10^8$  years, which is also close to the lifetime of the synchrotron emitting electrons, to the order of  $10^{44} \text{ erg s}^{-1}$ , consistent with our estimate. The very characteristic sharp outer boundary of the outer radio halo of M87, noted by Owen et al. (2000), has the important implications, that this could not have been produced by magnetic field advection in a cooling flow.

Thus, we find a radio structure providing evidence for a power input from the central AGN into the halo region of the order of about ten times the radiative energy loss rate over at least about  $10^8$  years (for M87). The energy input could therefore balance the heating for at least about  $10^9$  years. The observation of active AGN in the centers of cooling flows is a very common phenomenon. E.g., Ball et al. (1993) find in a systematic VLA study of the radio properties of cD galaxies in cluster centers, that 71% of the cooling flow clusters have radio loud cDs compared to 23% of the non-cooling flow cluster cDs. Therefore we can safely assume that the current episode of activity was not the only one in the life of M87 and its cooling flow.

The mechanism for a fine-tuned heating of the cooling

flow region should most probably be searched for in a feeding mechanism of the AGN by the cooling flow gas. The most simple physical situation would be given if simple Bondi type of accretion from the inner cooling core region would roughly provide the order of magnitude of the power output that is observed and required. Using the classical formula for spherical accretion from a hot gas by Bondi (1952) we can obtain a very rough estimate for this number. For the proton density near the M87 nucleus ( $r \leq 15''$ ) of about  $0.1 \text{ cm}^{-3}$ , a temperature of about  $10^7 \text{ K}$  (e.g., Matsushita et al. 2001), and a black hole mass of  $3 \times 10^9 M_{\odot}$  (e.g., Ford et al. 1994) we find a mass accretion rate of about  $0.01 M_{\odot} \text{ yr}^{-1}$  and an energy output of about  $7 \times 10^{43} \text{ erg s}^{-1}$ , where we have assumed the canonical value of 0.1 for the ratio of the rest mass accretion rate to the energy output. The corresponding accretion radius is about  $50 \text{ pc}$  ( $\sim 0.6''$ ). This accretion rate is more than a factor of 1000 below the Eddington value and thus no reduction effects of the spherical accretion rate by radiation pressure has to be expected. Small changes in the temperature and density structure in the inner cooling core region will directly have an effect on the accretion rate. Therefore we have all the best prospects for building a successful self-regulated AGN-feeding and cooling flow-heating model.

### 5. Implications of the AGN Cooling Flow Interaction

The contribution by Churazov in these proceedings describes in more detail the interaction scenario of the AGN with the central intracluster medium. In this new perspective the cooling cores of galaxy clusters become the sites where most of the energy output of the central cluster AGN is finally dissipated. Strong cooling flows should therefore be the locations of AGN with the largest mass accretion rates. While in the case of M87 with a possible current mass accretion rate of about  $0.01 M_{\odot} \text{ yr}^{-1}$  the mass addition to the black hole (with an estimated mass of about  $3 \times 10^9 M_{\odot}$ ) is a smaller fraction of the total mass, the mass build-up may become very important for the formation of massive black holes in the most massive cooling flows, where mass accretion rates above  $0.1 M_{\odot} \text{ yr}^{-1}$  become important over cosmological times.

### 6. Metal Abundance Peaks in Cooling Cores

Since the discovery of the iron emission line in the thermal spectra of the intracluster medium (ICM) in clusters of galaxies, the abundances of the heavy elements in the ICM have been an important diagnostics of the cluster formation history in particular for the star formation history in the cluster volumina. The large amount of iron implied that the cluster galaxies must have lost a large fraction of the iron produced during their star formation histories to the ICM due to galactic winds. The total iron mass in the ICM is in fact larger than the total iron mass in all cluster galaxies.

Here we concentrate on the implications of the heavy element abundances in the central regions. With the ASCA satellite observatory which provided the first possibility of spatially resolved spectroscopy of the cluster ICM it was found that some clusters with cD galaxies

had a strong increase in the metal abundance towards the center (e.g., Fukazawa et al. 1996, 1998, Matsumoto et al. 1996, Ikebe et al. 1999). With similar results from BeppoSAX with slightly better spatial resolution DeGrandi and Molendi (2001) showed that these iron abundance peaks are a signature of cooling core clusters. Again with observational data from ASCA, Finoguenov et al. (2000) could derive abundance profiles of Fe and Si and could show that the central regions in those clusters with metal abundance peaks were strongly enriched in iron while the bulk volume of the clusters outside the central region had an iron-to-silicon ratio close to the yields of SN type II. This implies that the central excess seen in cooling core clusters is most probably due to enrichment by SN type Ia in the cD galaxies in the recent past, during which the central region of the cluster was not disturbed.

Now with recent XMM-Newton observations of M87 (Böhringer et al. 2001, Matsushita et al. 2002, 2003a) we have a detailed picture of the radial abundance profiles for the M87 halo region in the center of the Virgo cluster of the seven diagnostically important elements, O, Mg, Si, S, Ar, Ca, Fe. They provide a finger print of the origin of the metals: less than about 10% (contribution an iron abundance of roughly 0.15 in solar units) of the iron in the central region is produced by SN II and most of the metals comes from more recent SN Ia (Finoguenov et al. (2001). The SN II abundance contribution in the center of Virgo can also be compared to the iron abundances in the outer regions of clusters, where SN II enrichment dominates (Finoguenov 2000, DeGrandi & Molendi 2001). In these outer regions we find typical iron abundances of about 0.2 of the solar value, roughly consistent with the above number. Thus the central iron abundance peaks are due to recent SN Ia enrichment from the central dominant elliptical galaxies.

### 7. Iron Mass Contained in the Abundance Peak

To further explore the significance of the central abundance peaks we calculate the total iron mass profiles,  $M_{Fe}(\leq r)$ , for the clusters Virgo, Centaurus, Perseus, and A1795 from the gas mass profiles and the Fe abundance profiles as given by Matsushita et al. (2002, 2003a, 2003b), Churazov et al. (2003), Ikebe et al. (2003), respectively. The results in Fig. 4 show as dashed lines the total Fe mass profiles and as solid lines the profiles for the iron abundance excess, where an ubiquitous Fe abundance of 0.2 of the solar value was subtracted. As shown in Fig. 4 the widely distributed Fe component is a truly minor fraction inside a radius of, e.g., 50 kpc.

We note that the iron masses in the abundance excess are quite large. Inside 10 kpc, a radius that is for example of the order of the scale radius of the giant elliptical galaxies, we find masses of the central iron excess from several  $10^6$  to several  $10^7 M_{\odot}$ . The values have a spread of about one order of magnitude. At a radius of 50 kpc, where in terms of the total stellar light the central galaxy is still completely dominant, the spread becomes significantly smaller and the total iron mass inside this radius ranges from  $1.5$  to  $3 \times 10^8 M_{\odot}$ .

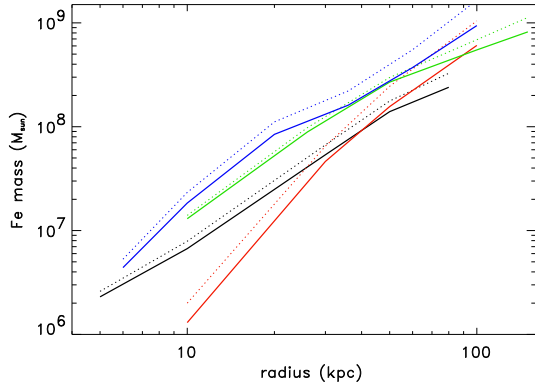


FIG. 4.— Cumulative iron mass profiles in the centers of the galaxy clusters M87/Virgo (black), Centaurus (green), Perseus (red) and A1795 (blue). The dashed lines show the total iron mass and the solid lines show the iron mass in the central excess where a mean abundance of 0.2 solar was subtracted.

## 8. Enrichment Ages for cD Halos in Galaxy Clusters

To better understand the enrichment and transport processes in these environments we introduce the concept of enrichment time of the central ICM. We take iron as the enrichment tracer and define the time with respect to the enrichment of iron.

We assume that Fe is introduced into the ICM by (a) input from SNIa explosions and (b) by stellar mass loss from a stellar population heavily enriched in Fe (about 2 times the solar value). For the SNIa enrichment we assume a supernova rate of 0.15 SNU, a value slightly larger than that of Capellaro et al. (1999; 1SNU corresponds to a rate of  $10^{-2} \text{ yr}^{-1}$  per  $10^{10} L_{B\odot}$ ). The stellar mass loss is estimated to be about  $2.5 \times 10^{-11} L_B$  (Ciotti et al. 1991 – assuming a galactic age of 10 Gyr) and the stellar iron abundance is taken as roughly twice solar. With rough estimates of radial light profiles of the central galaxies we can calculate the necessary time to produce the iron inside a certain radius as given in the iron mass profiles for the excess abundance in Fig. 4. Fig. 5 shows the necessary enrichment times. We note that the large iron masses observed require long enrichment times, such that at a radius of 50 kpc times of 20 Gyr and more are required, that is times larger than the age of the Universe.

In these calculations we have not yet accounted for the fact that the SNIa rate is expected to be larger in the past for a younger stellar population. Also the stellar mass loss will be larger at earlier epochs. The evolution of these enrichment rates,  $R(t)$ , is often modeled by a power law behavior (e.g., Renzini et al. 1993). Using a relatively strong evolution we tentatively model the change of the SNIa rate together with the smaller contribution from stellar mass loss by a power law

$$R(t) = R_0 \left( \frac{t}{t_0} \right)^{-s}$$

where  $s$  is taken to be 2 ( $T_0 = 13$  Gyr). The results for the so determined enrichment times is shown in Fig.

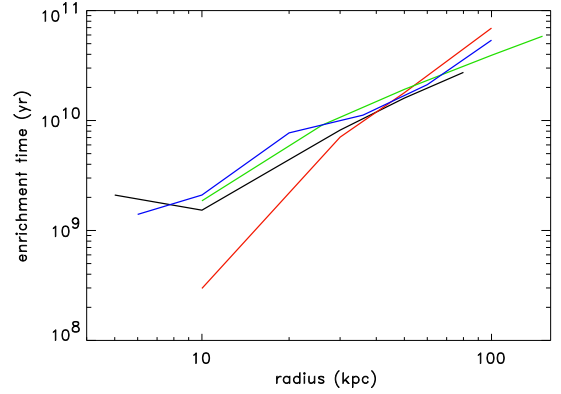


FIG. 5.— Enrichment ages of the central iron abundance peak in the galaxy clusters M87/Virgo (black), Centaurus (green), Perseus (red) and A1795 (blue). The enrichment times were calculated on the basis of a SN Ia rate of 0.15 SNU (Capellaro et al. 1999) and an additional contribution by stellar mass loss.

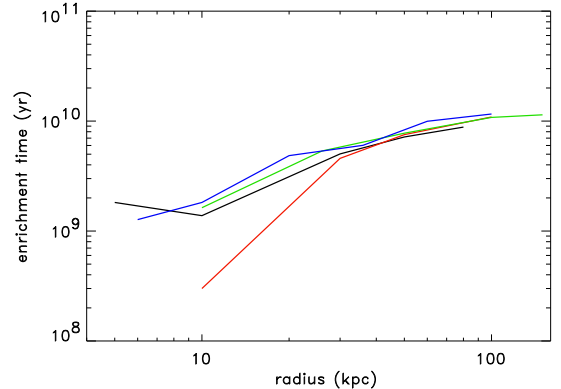


FIG. 6.— Enrichment ages of the central iron abundance peak in the galaxy clusters M87/Virgo (black), Centaurus (green), Perseus (red) and A1795 (blue). The enrichment times were calculated on the basis of a SN Ia rate of 0.15 SNU for the present time and an increase of the rate in the past (see text).

6. The enrichment times for large radii are now converging to times around  $10^{10}$  Gyr. In this model the most important contribution at large radii is happening at the earliest times, which results in the flattening of the curves. At a radius of 50 kpc the different examples converge to a surprisingly narrow age span of 7–8.5 Gyr.

## 9. Implications for Cluster Cooling Flows

Turning again to the classical cooling flow picture, we can with the given observed parameters and with the known mass deposition profiles calculated in the classical way for cooling flow models (e.g., Allen et al. 2001, Matsushita et al. 2002, Ikebe et al. 2003, Churazov et al. 2003) determine the iron mass loss rate from the ICM due to mass deposition for a steady state situation and the given abundances. We find that iron would be lost in classical inhomogeneous cooling flows by factors of 4 to 12 faster than it could be replenished for the given abundance distribution at a radius of 10 kpc. At the larger radius of 50 kpc the difference is even a factor 6 - 45 for the four cases. Therefore it seems very difficult to sustain the very large central iron concentrations in the frame of

the cooling flow mass deposition model. If the cooling flow model would not have been abandoned due to inconsistency with spectroscopic observations, this would be another conflict for this model.

### 10. Implications for Other ICM Transport Histories

The long enrichment times do not only have implications for cooling flow models, but they put constraints on any disturbances of the central regions of the clusters. Such disturbances could for example be provided by the proposed heating models of cooling core regions by AGN. If, e.g., the heating model by bubbles of relativistic plasma from radio lobes, as proposed by Churazov et al. (2000, 2001), leads to a large convective motion covering the full cooling core region, gas could be transported around in a circle in a few Gyr. This would tend to flatten the observed steep abundance profiles. Numerical simulations as performed, e.g., by Brüggén (2002) where the effect of buoyantly rising bubbles was studied in the presence of tracer particles show that the convection induced in the ambient gas by the relativistic plasma bubbles may be more “differential”, such that individual gas parcels are only dragged along for shorter distances. Such a gentle motion would be consistent with the observed metallicity profiles. In fact some transport of the iron from the central galaxy out to radii larger than 50 kpc is required, since the iron mass excess distribution is more extended than the stellar population of the central galaxy.

The fact that the enrichment time in the central region in Perseus is much smaller than for the other clusters suggests the interpretation that the central region of Perseus may be more stirred than that of the other clusters. Indeed the present power output of the central galaxy NGC1275 as deduced from the radio lobe interaction effects averaged over the last few  $10^7$  yr (Churazov et al. 2000) is with a power of about  $10^{45}$  erg  $s^{-1}$  larger than for the other clusters and thus the deviating properties of the central region of Perseus may thus find a very natural explanation. At larger radii the iron mass profile and the enrichment times for this cluster are not very different from the other examples. Strong turbulent motion of the gas in the center of the Perseus cluster is also implied by recent work of Churazov et al. (2003) from the absence of effects of resonant line scattering in the Fe  $K\alpha$  to  $K\beta$  ratio.

Finally the observations also put strong constraints on the effects of cluster mergers on the cooling cores of clusters. Traditionally cluster mergers are believed to destroy cooling flows (e.g., McGlynn & Fabian 1984). Allen et al. (2001) have calculated cooling flow ages on the basis of the comparison of the spectroscopically inferred mass flow rates with those rates determined from the surface brightness distribution and finds cooling flow ages of the order of a few to several Gyr. This is consistent with the merger frequency expected to be a few Gyr (e.g., Schuecker et al. 2001). The above analysis suggests that the cooling cores are in general older than the time to the last major merger. This implies that most mergers do not destroy the cooling cores. The disturbance of cooling cores by mergers may therefore just result in a sloshing motion of the dense gaseous core as observed in the form of frequently observed cold fronts (e.g., Markevitch et al. 2000) which may not lead to a destruction of the cores. The difficulty of destroying the cluster core by a cluster merger was, e.g., pointed out by Churazov et al. (2003) who analyzed the signatures of the sloshing motion of the cooling core in the Perseus cluster from recent XMM-Newton data.

### 11. Summary and Conclusions

The large metal abundance excesses in cooling core regions of clusters of galaxies indicate that large enrichment times are necessary to create them. For the four examples studied here, the Virgo, Perseus, Centaurus, and Abell 1795 clusters, we find enrichment times of 7 - 10 Gyrs for the central 50 kpc radius region. Thus we conclude that the dense cooling cores in clusters are very persistent phenomena. They have been formed very early in the clusters studied here and must have survived cluster mergers as well as the possible convective motions induced by the buoyantly rising relativistic plasma expelled by the central AGN of the central cluster galaxies.

These studies can easily be expanded to a larger sample of clusters to test if these conclusions hold in general. But since very similar abundance gradients are observed for most cooling core clusters we expect that this will be the case. The extensive XMM-Newton observations conducted and planned will strongly enhance our understanding of these phenomena.

### References

- Sarazin, C. L. 1988, X-ray Emissions from Clusters of Galaxies (Cambridge: Cambridge Univ. Press)
- Allen, S.W., 2000, MNRAS, 315, 269
- Allen, S.W., Fabian, A.C., Johnstone, R.M., et al., 2001, MNRAS, 322, 589
- Ball, R., Burns, J.O., Loken, C., 1993, AJ, 105, 53
- Bertschinger, E. & Meiksin, A., 1986, ApJ, 306, L1
- Böhringer, H., Voges, W., Fabian, A.C. Edge, A.C., and Neumann, D., 1993, MNRAS, 264, L25
- Böhringer, H., Belsole, E., Kennea, J., et al., 2001, A&A, 365, L181
- Böhringer, H., Matsushita, K., Churazov, E., Ikebe, Y., Chen, Y., 2002, A&A, 382, 807
- Böhringer, H., 2003, Reviews in Modern Astronomy, in press
- Bondi, H., 1952, MNRAS, 112, 195
- Brüggén, M., 2002, ApJ, 571, 10
- Churazov, E., Forman, W., Jones, C., Böhringer, H., 2000, A&A, 356, 788
- Churazov, E., Brüggén, M., Kaiser, C.R., Böhringer, H., & Forman, W., 2001, ApJ, 554, 261
- Churazov, E., Sunyaev, R., Forman, W., Böhringer, H., 2002, MNRAS, 332, 729
- Churazov, E., Forman, W., Jones, C., Böhringer, H., 2003, ApJ, 590, 225
- De Grandi, S., & Molendi, S., 2001,
- Ezawa, H., Fukazawa, Y., Makishima, K., Ohashi, T., Takahara, F., Xu, H., Yamasaki, Y., 1997, ApJ, 490, L33
- Fabian, A.C., 1994, ARA&A, 32, 277

- Fabian, A. C., Sanders, J. S., Ettori, S., et al. 2000, MNRAS 318, 65
- Fabian, A.C., Mushotzky, R.F., Nulsen, P.E.J., Peterson, J.R., 2001, MNRAS, 321, 20
- Finoguenov, A., David, L.P., Ponman, T.J., 2000, ApJ, 514, 188
- Finoguenov, A., Arnaud, M., David, L.P., 2001a, ApJ, 555, 191
- Finoguenov, A., Matsushita, K., Böhringer, H., Ikebe, Y., Arnaud, M., 2002a, A&A, 381, 21
- Finoguenov, A., Jones, C., Böhringer, H., Ponmann, T.J., 2002b, ApJ, 578, 74
- Fukazawa, Y., Makishima, K., Matsushita, K., Yamasaki, N., Ohashi, T., Mushotzky, R.F., Sakima, Y., Tsusaka, Y., Yamashita, K., 1996, PASJ, 48, 395
- Fukazawa, Y., Makishima, K., Tamura, T., Ezawa, H., Xu, H., Ikebe, Y., Kikuchi, K., Ohashi, T., 1998, PASP, 50, 187
- Ford, H.C., et al. 1994, ApJ, 435, L27
- Ikebe, Y., Makishima, K., Fukazawa, Y., et al., 1999, ApJ, 525, 58
- Kaastra, J.S., Tamura, T., Peterson, J.R., et al., 2003, A&A in press, astro-ph/0309763
- Kassim, N., Perley, R.A., Erickson, W.C., Dwarakanath, K.S., 1993, AJ, 106, 2218
- Makishima, K., Ezawa, H., Fukazawa, Y., et al., 2001, PASJ, 53, 401
- Matsumoto, H., Koyama, K., Awaki, H., Tomida, H., Tsuru, T., 1996, PASP, 48, 201
- Matsushita, K., Belsole, E., Finoguenov, A., Böhringer, H., 2002, A&A, 386, 77
- Matsushita, K., Finoguenov, A., Böhringer, H., 2003a, A&A, 401, 443
- Matsushita, K. et al., 2003b, A&A, submitted
- McNamara, B., Wise, M., Nulsen, P.E.J., et al. 2000, ApJ, 534, L135
- Molendi, S. & Pizzolato, F., 2001, ApJ, 560, 194
- Molendi, S. & Gastaldello, F., 2001, A&A, 375, L14
- Nulsen, P.E.J., 1986, MNRAS, 221, 377
- Owen, F.N., Eilek, J.A., Kassim, N.E., 2000, ApJ, 543, 611
- Pedlar, A., Ghataure, H. S., Davies, R. D., et al., 1990, MNRAS, 246, 477
- Peterson, J.R., Paerels, F.B.S., Kaastra, J.S., et al., 2001, A&A, 365, L104
- Renzini, A., Ciotti, L., D'Ercole, A., Pellegrini, S., 1993, ApJ, 419, 52
- Renzini, A., 1997, ApJ, 488, 35
- Rottmann, H., Mack, K.-H., Klein, U., Wielebinski, R., 1996, A&A, 309, L9
- Soker, N. & Sarazin, C.L., 1990, ApJ, 348, 73
- Tabor, G. & Binney, J., 1993, MNRAS, 263, 323
- Tamura, T., Kaastra, J.S., Peterson, J.R., et al., 2001, A&A, 365, L87
- Tucker, W.H. & Rosner, R., 1983, ApJ, 267, 547
- Thomas, P.A., Fabian, A.C., & Nulsen, P.E.J., 1987, MNRAS, 228, 973